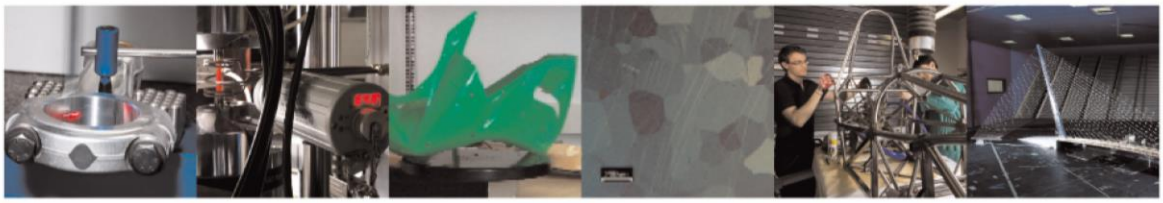

Spheroidizing annealing of thermomechanically hot-rolled steel rods: influence of the prior microstructure on the mechanical characteristic and phase transformations

B. Rivolta, R. Gerosa, D. Panzeri, L. Piazza, L. Angelini, M. Alfonso, N. Bolognani, A. Panzeri, A. Parimbelli, C. Sala

This manuscript has been accepted for publication in Ironmaking & Steelmaking. This is the author accepted manuscript (AAM), and it has not been copyedited or formatted for final publication.
Spheroidizing annealing of thermomechanically hot-rolled steel rods: influence of the prior microstructure on the mechanical characteristic and phase transformations
B. Rivolta, R. Gerosa, D. Panzeri, L. Piazza, L. Angelini, M. Alfonso, N. Bolognani, A. Panzeri, A. Parimbelli, and C. Sala, Ironmaking & Steelmaking 2022 49:7, 716-725.

DOI: https://doi.org/10.1080/03019233.2022.2049582

Spheroidizing annealing of thermomechanically hot-rolled steel rods: influence of the prior microstructure on the mechanical characteristic and phase transformations

B. Rivolta, R. Gerosa, D. Panzeri, L. Piazza - Politecnico di Milano, Dipartimento di Meccanica, Milano

L. Angelini, M. Alfonso, N. Bolognani, A. Panzeri, A. Parimbelli, C. Sala - Caleotto S.p.A., Lecco

Abstract

High deformability is a very important property especially when severe cold plastic deformations are required. The hot-rolled wire rod represents the raw material for drawing and forging operations. The deformability of such steels depends on the microstructure strongly and the effort of many companies to modify the microstructure of the as-rolled product is hence justified. Nevertheless, a following spheroidizing annealing is commonly carried out to decrease the mechanical resistance and increase the deformation capability. On the other hand, high spheroidization of the carbides can have effects on the austenitization kinetics during the quenching. In this work, the influence of heat treatments at 690 °C and 720 °C was studied on a low-carbon boron steel. Microstructure and mechanical characteristics were studied varying the soaking time. Different prior microstructural conditions were obtained modifying the thermo-mechanical rolling and the Stelmor cooling parameters. Other microstructural conditions were prepared by laboratory heat treatments. The results remarked the importance of the prior microstructure on the shape and the distribution of the carbides after spheroidizing. Moreover, also the spheroidization rate was influenced by the prior microstructure. In fact, in comparison with the ferritic and pearlitic condition, the bainitic and the martensitic ones resulted in a faster and more uniform dispersion of the carbides. Regarding the pearlitic microstructures, the finest structure, obtained by a suitable thermo-mechanical rolling, showed a more homogeneous distribution of the carbides.

Keywords. Microstructure; thermomechanical rolling; spheroidization treatment; deformability

1. Introduction

The production of high-strength components, such as bolts and fasteners, often involves low-carbon boron steels because of their cold formability and their good hardenability due to the boron addition [1,2]. After the hot rolling, drawing and forging operations are usually carried out to obtain the final geometry. Finally, after the shaping process, quenching and tempering are usually performed to obtain the desired mechanical characteristics. Nevertheless, for specific products such as long bolts and fasteners, distortions can occur after quenching because of the fast cooling. This deformation is sometime excessive and can lead to the discard of the part. For such a reason, the industrial research is working on the microstructure after hot rolling to obtain a good combination of strength and deformability, sufficient to support the plastic strains imposed by the cold-deformation stage. The combination of thermomechanical hot rolling and Stelmor cooling could give the best microstructure for the successive manufacturing steps [3,4]. In any case, when the geometry of a component requires very high and localized strains, the deformability shall be increased as much as possible. This is obtained by suitable heat treatments after hot rolling, such as the spheroidizing annealing [5]. This process causes a huge modification on the material microstructure, resulting in a mechanical softening and in an increase of the deformation capability. Because of the long soaking times at temperatures close to the A_1 phase-transformation temperature, pearlitic microstructures are modified into a ferritic matrix with a dispersion of carbides. The shape and the distribution of such particles influence the steel formability [7]. For all these reasons, plants involving thermomechanical rolling and the possibility to control the cooling rate (for example by mean of the Stelmor conveyor), are particularly suitable for the development

of innovative products. The present experimental work aims to study the mechanical properties of different microstructures produced by Stelmor cooling after conventional and thermomechanical rolling in the as-produced and the annealed conditions. The technical literature [5,6,7,8,9,10,11,12,13], in fact, shows that the spheroidization rating and kinetics can be influenced by the prior microstructure. The spheroidizing temperatures were selected after a preliminary dilatometric analysis of the as-produced standard condition, in order to determine both the A_3 and the A_1 phase-transformation temperatures: the second one is particularly important, since the spheroidizing treatment must be done as close as possible to such value. For C-Mn-B steels, typical annealing temperatures range between 680 °C and 730 °C. As known, higher temperatures speed up the process and generate coarser carbides that increase the deformability, even if they can make the $\alpha \rightarrow \gamma$ transformation during the quenching slower [14,15]. This issue will be investigated as well by dilatometry varying the initial microstructure. To find a satisfying compromise among deformability and response to the following heat treatment, lower spheroidizing temperatures can be considered. In the present work, the authors focused the attention on the hardness and the tensile properties of specimens treated at 690 °C and 720 °C for different soaking times.

2. Materials and methods

The material under investigation is a 10 mm diameter wire rod produced by hot rolling. The nominal chemical composition is reported in Table 1.

Element	**C**	**Mn**	**Si**	**S**	**P**	**B**	**Ti**
wt. %	0.25	0.88	0.13	0.004	0.014	0.004	0.045

Table 1. Nominal chemical composition in wt. % of the investigated steel.

Different microstructures were obtained both modifying the Stelmor cooling parameters after conventional and thermo-mechanical hot rolling, both by laboratory heat treatments.

Industrial heat treatments			
C	Conventional rolling	Temperature at the laying head: 870 °C	Cooling under insulating hoods
TMR	Thermomechanical rolling	Temperature at the laying head: 820 °C	Cooling under insulating hoods
TMR-S	Thermomechanical rolling	Temperature at the laying head: 820 °C	Forced air cooling

Table 2. Industrial heat treatments.

Laboratory heat treatments		
A	Austenitization: 900 °C, 25 min	Furnace cooling
Q	Austenitization: 900 °C, 25 min	Water cooling

Table 3. Laboratory heat treatments.

The thermomechanical rolling involves a final deformation stage at about 820 °C. Such temperature is obtained thanks to a cooling loop before the wire rod enters the last rolling block.

The phase-transformation temperatures were determined by dilatometry. According to the ASTM E228 − 17 standard, the heating rate was equal to 2 K/min. On the base of the A_1 value, the spheroidizing treatments were carried out in a laboratory furnace at 690 °C and 720 °C for different times ranging from 1 h to 12 h. For all the conditions, the cooling was performed at about 18 °C/min until 500 °C and then in still air to room temperature. The obtained microstructures were observed and documented by the standard metallographic technique, whereas the mechanical properties were determined by hardness and tensile tests on wire rod specimens 300 mm long.

3. Experimental results

3.1 Dilatometric and microstructural analysis

The dilatometric tests were performed on a push-rod Netzsch DIL 402 E dilatometer under a protective atmosphere of N_2 + 5 % H_2 to prevent the specimen oxidation. Figure 1 shows the obtained dilatometric curve for the conventionally rolled material (condition C). The phase transformations can be identified studying the curve first derivative: a decrease of the slope occurs when the $\alpha \rightarrow \gamma$ transformation starts (A_1), while a new increase remarks the end of the transformation (A_3). The obtained values are A_1 = 735 °C and A_3 = 835 °C.

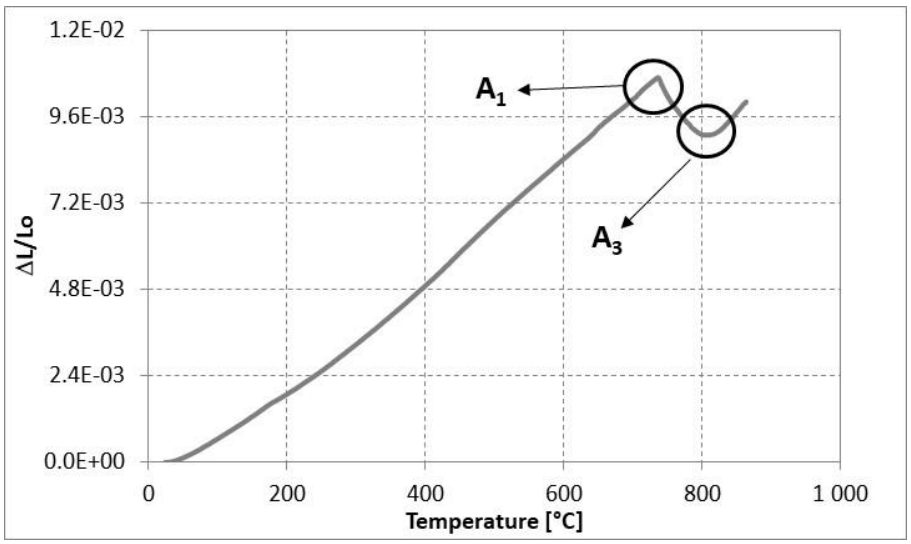

Figure 1. Dilatometric curve obtained on the conventionally rolled material.

A wide microstructural survey by LOM and SEM was carried out to characterize the steel after the industrial and the laboratory treatments both before and after the spheroidizing annealing at 690 °C and 720 °C for 1 h, 3 h, 6 h and 12 h. The microstructure after the industrial, the laboratory heat treatments and after a soaking at 720 °C and 690 °C for 12 h are presented in Figure 2. Higher magnifications were obtained by SEM as shown in Figures 3 and 4.

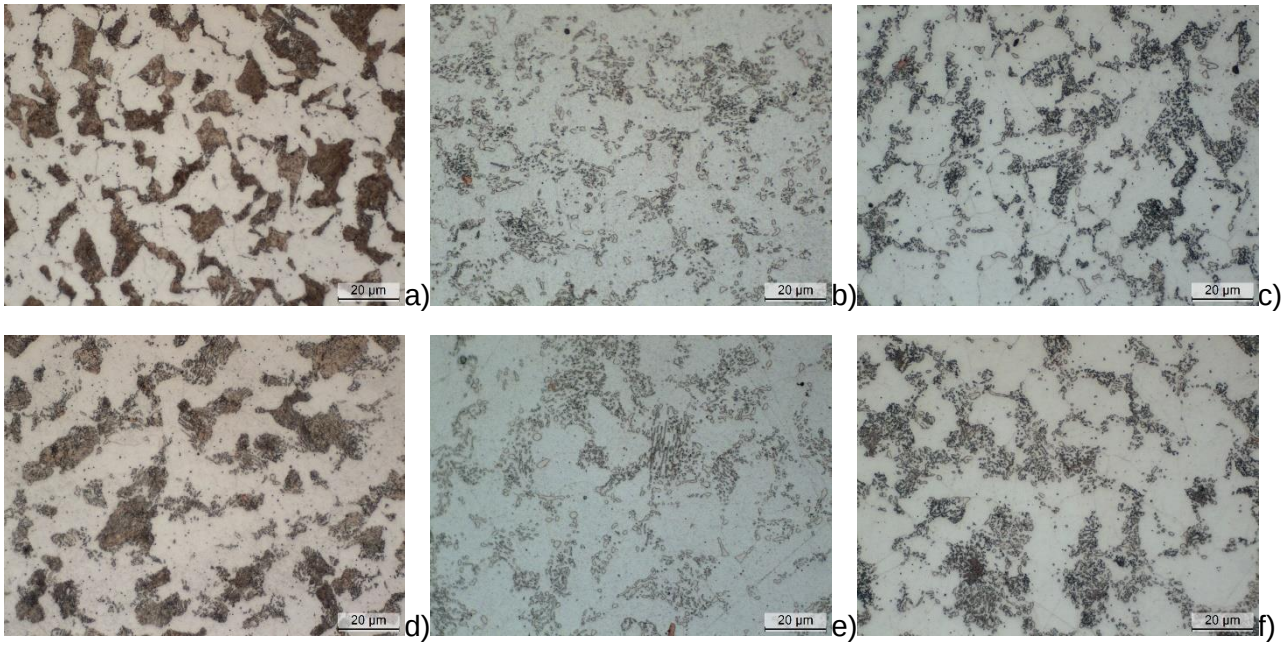

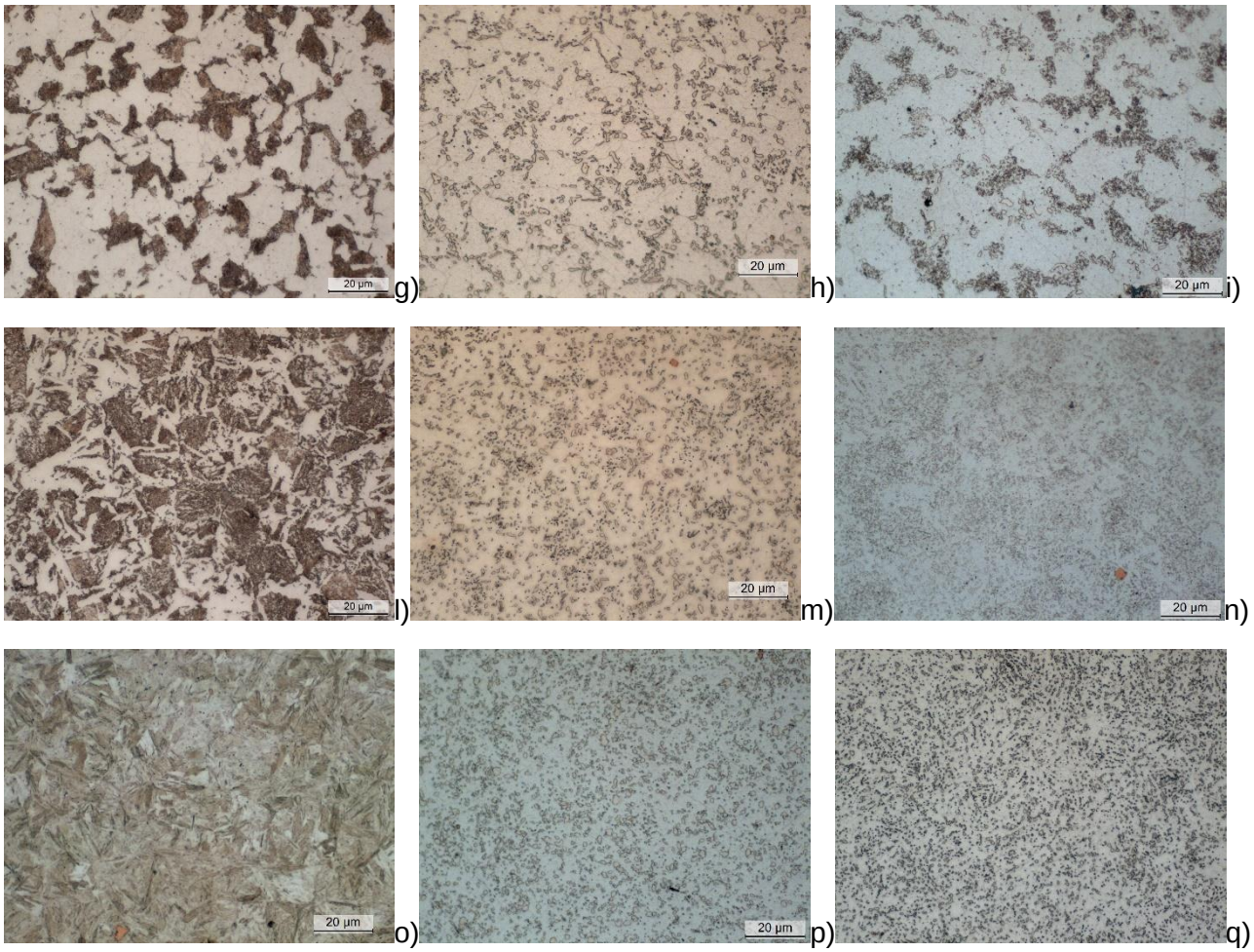

Figure 2. Microstructure observed in as-produced C (a), A (d), TMR (g), TMR-S (l), Q (o) specimens (left column), in 720 °C, 12 h treated C (b), A (e), TMR (h), TMR-S (m), Q (p) specimens (center column) and in 690 °C, 12 h treated C (c), A (f), TMR (i), TMR-S (n), Q (q) specimens (right column).

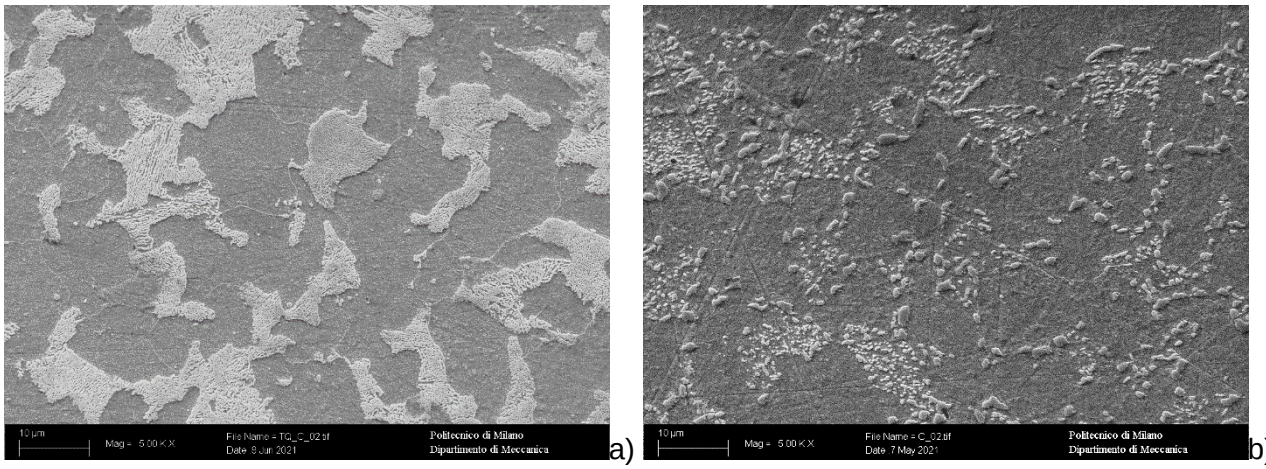

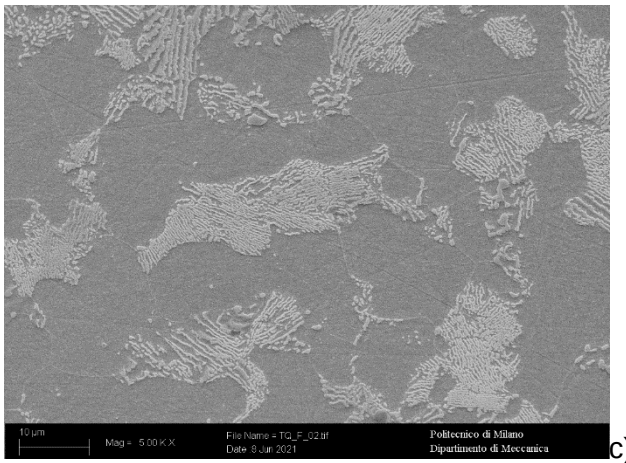
10 µm
Mag = 5.00 K X
File Name = TG_F_02.tif
Date :8 Jun 2021
Politecnico di Milano
Dipartimento di Meccanica

c)

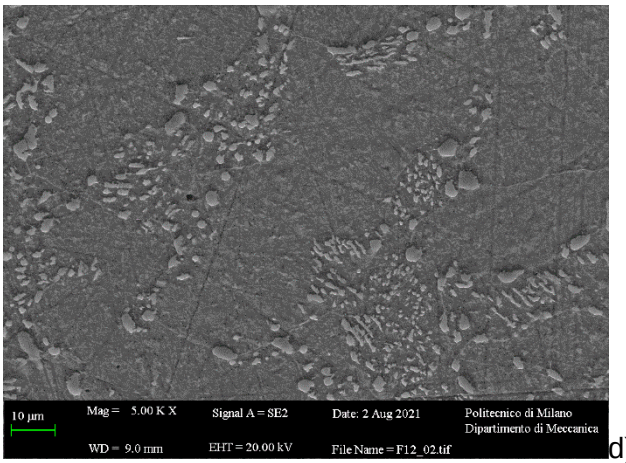
10 µm
Mag = 5.00 K X
Signal A = SE2
Date: 2 Aug 2021
Politecnico di Milano
Dipartimento di Meccanica
WD = 9.0 mm
EHT = 20.00 kV
File Name = F12_02.tif

d)

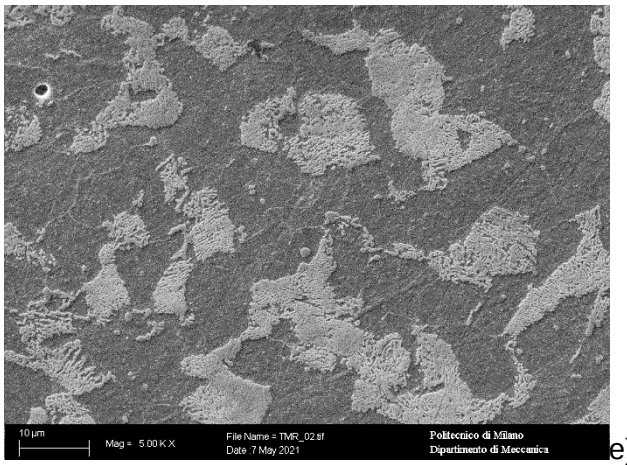
10 µm
Mag = 5.00 K X
File Name = TMR_02.tif
Date :7 May 2021
Politecnico di Milano
Dipartimento di Meccanica

e)

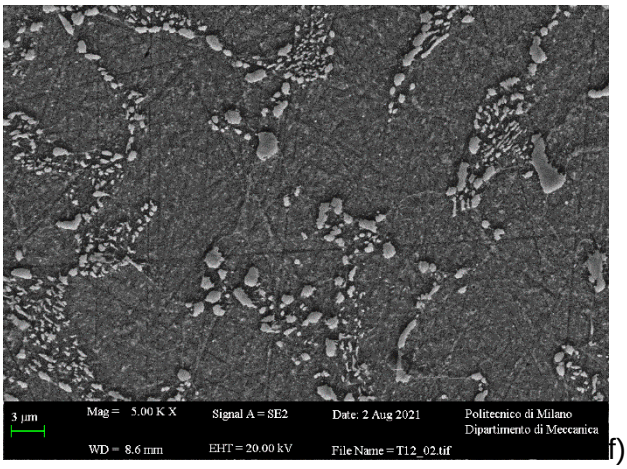
3 µm
Mag = 5.00 K X
Signal A = SE2
Date: 2 Aug 2021
Politecnico di Milano
Dipartimento di Meccanica
WD = 8.6 mm
EHT = 20.00 kV
File Name = T12_02.tif

f)

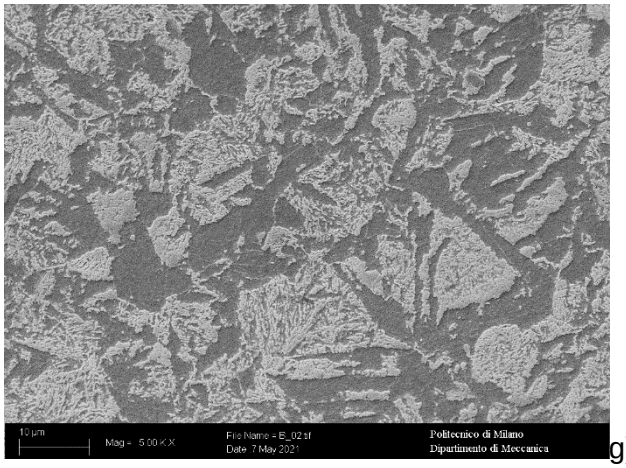
10 µm
Mag = 5.00 K X
File Name = B_02.tif
Date :7 May 2021
Politecnico di Milano
Dipartimento di Meccanica

g)

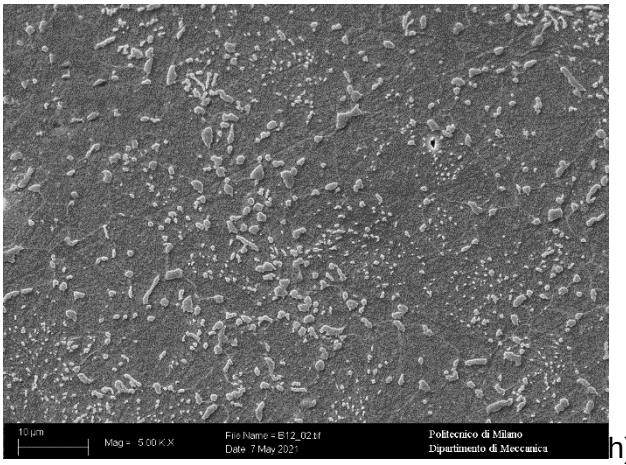
10 µm
Mag = 5.00 K X
File Name = B12_02.tif
Date :7 May 2021
Politecnico di Milano
Dipartimento di Meccanica

h)

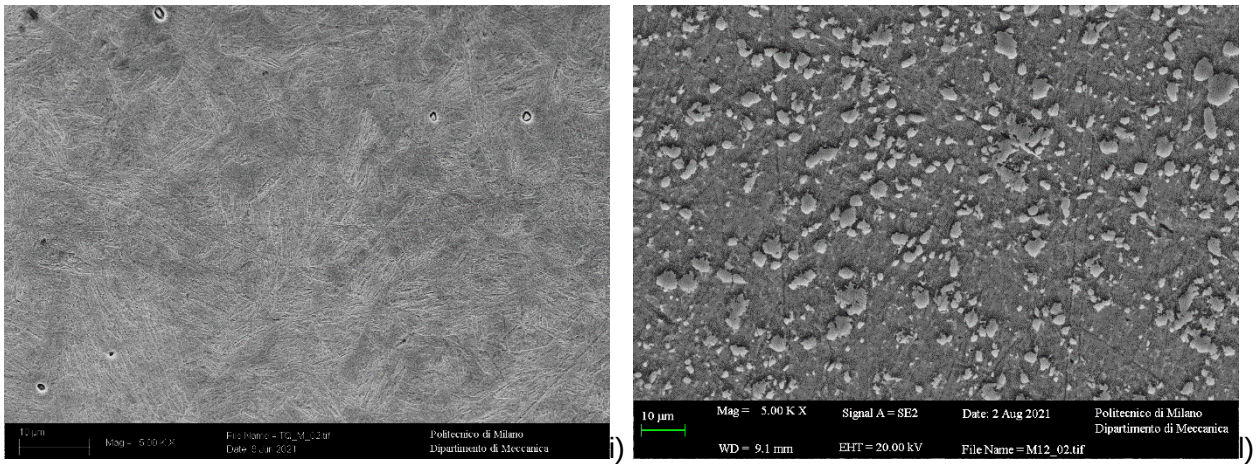

i) l)

Figure 3. Microstructure observed in as-produced C (a), A (c), TMR (e), TMR-S (g), Q (i) specimens and in 720 °C, 12 h treated C (b), A (d), TMR (f), TMR-S (h), Q (l) specimens.

The microstructure generated by slow cooling under insulated hoods (conditions C and TMR) is ferrite and pearlite, even if the thermomechanical rolling (condition TMR) induced a grain refinement and an increase of the ferrite fraction (from about 50 % for the conventionally rolled rod to about 60 % for the thermo-mechanical rolling). The microstructure obtained with a faster cooling (condition TMR-S) is instead characterized by a bainitic microstructure. Regarding the laboratory treatments, furnace cooling (condition A) generated a coarse ferritic and pearlitic microstructure, while the water cooling resulted in a fully martensitic matrix (condition Q). After 720 °C, 12 h treatment, most of the carbides are spheroidized even if some lamellar carbides are still visible especially in the specimens coming from the coarse pearlite microstructure (condition A) as visible in Figure 3 (d). The main difference among the micrographs in Figure 3 is the dispersion of the carbides after the spheroidizing treatment: when the carbon is well distributed in the metal matrix of the prior microstructure, like the bainitic and especially the martensitic conditions, the resulting carbides are arranged uniformly in the annealed samples [7]. Regarding the ferrite-pearlite conditions, finer microstructures result in a more homogeneous particles distributions and in smaller carbides clusters.

The specimens annealed at 690°C showed thinner and more clustered carbides and, for the ferrite-pearlite microstructures, higher residual amount of lamellar carbides. Nevertheless, the spheroidization rating after 12 h is anyway satisfying. Aiming to remark the effect of the annealing temperatures better, SEM images are compared in Figure 4.

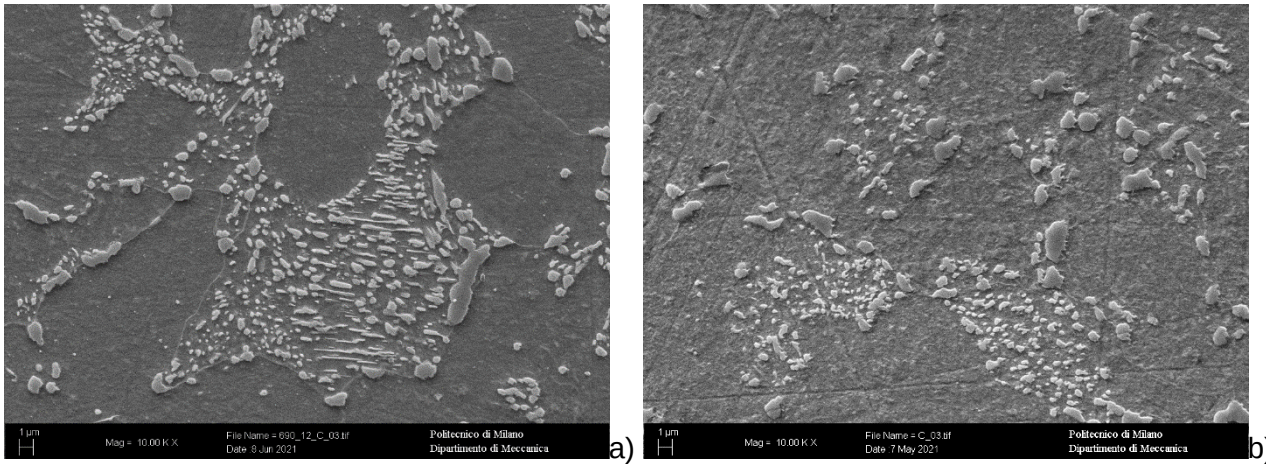

a) b)

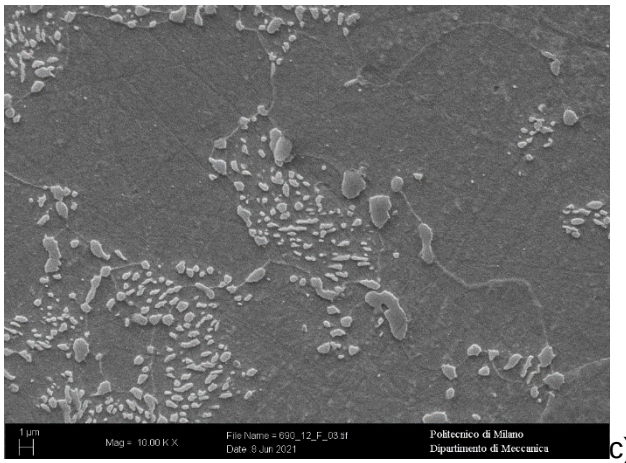
1 µm
Mag = 10.00 K X
File Name = 690_12_F_03.tif
Date 8 Jun 2021
Politecnico di Milano
Dipartimento di Meccanica
c)

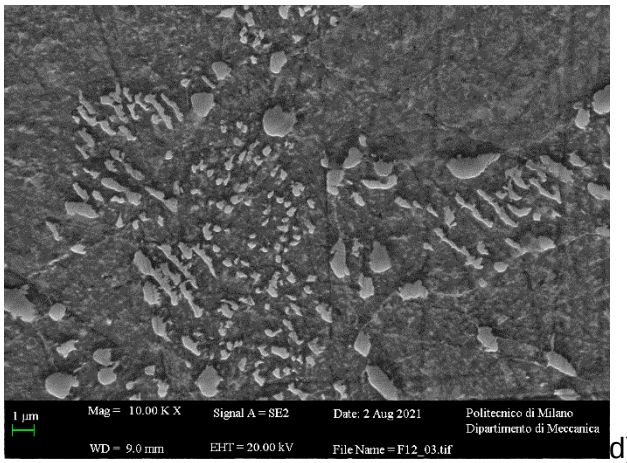
1 µm
Mag = 10.00 K X
Signal A = SE2
Date: 2 Aug 2021
Politecnico di Milano
Dipartimento di Meccanica
WD = 9.0 mm
EHT = 20.00 kV
File Name = F12_03.tif
d)

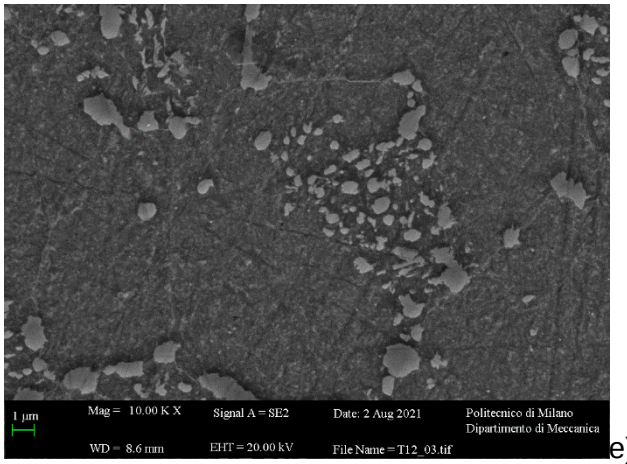
1 µm
Mag = 10.00 K X
Signal A = SE2
Date: 2 Aug 2021
Politecnico di Milano
Dipartimento di Meccanica
WD = 8.6 mm
EHT = 20.00 kV
File Name = T12_03.tif
e)

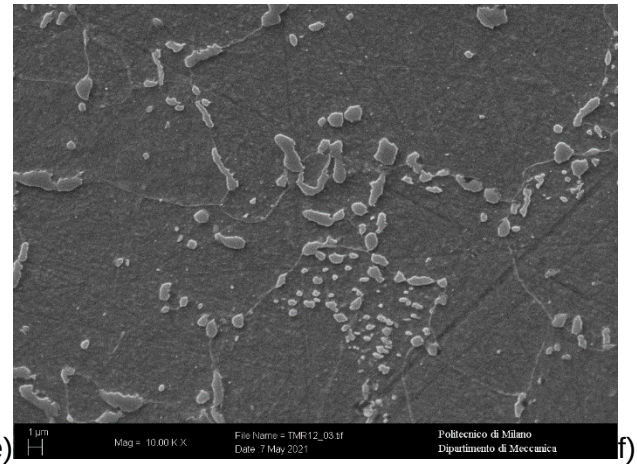
1 µm
Mag = 10.00 K X
File Name = TMR12_03.tif
Date 7 May 2021
Politecnico di Milano
Dipartimento di Meccanica
f)

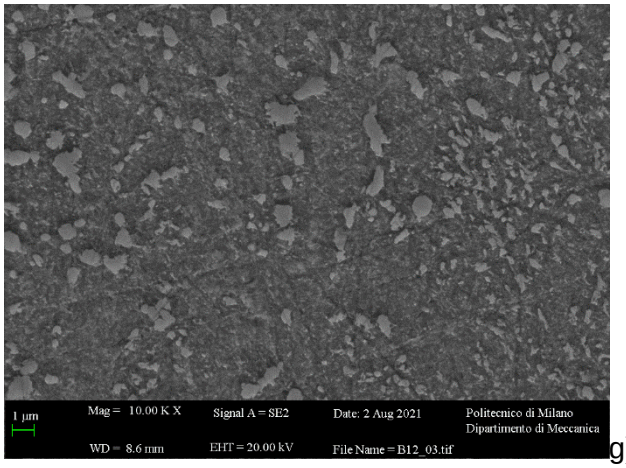
1 µm
Mag = 10.00 K X
Signal A = SE2
Date: 2 Aug 2021
Politecnico di Milano
Dipartimento di Meccanica
WD = 8.6 mm
EHT = 20.00 kV
File Name = B12_03.tif
g)

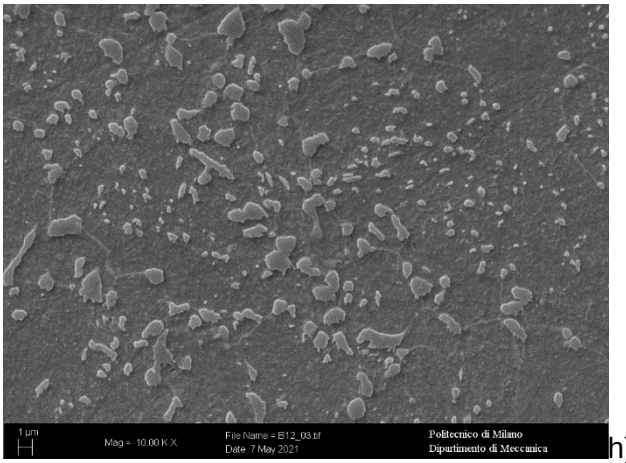
1 µm
Mag = 10.00 K X
File Name = B12_03.tif
Date 7 May 2021
Politecnico di Milano
Dipartimento di Meccanica
h)

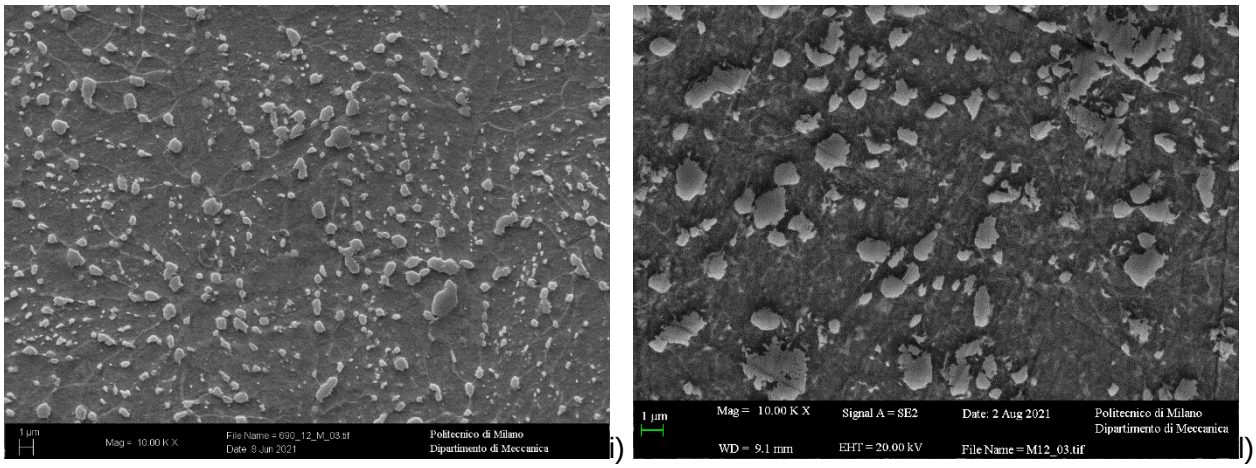

i) l)

Figure 4. Microstructure observed in 690 °C, 12 h soaking C (a), A (c), TMR (e), TMR-S (g), Q (i) specimens (left column) and in 720 °C, 12 h treated C (b), A (d), TMR (f), TMR-S (h), Q (l) specimens (right column).

As said in the previous paragraph, rounded carbides can slow down the austenitization kinetics during the quenching treatment. Aiming to study such phenomenon more deeply, dilatometric tests were performed on specimens in the as-produced condition and after spheroidizing treatment at 720 °C, 12 h to compare the corresponding $\alpha \rightarrow \gamma$ transformations. To clarify the influence of the prior microstructure, ferritic and pearlitic (conditions C and TMR) and martensitic (condition Q) matrixes were considered. The austenite fraction at each time during the transformation was determined from the dilatometric curve according to the procedure described by Huiping Li et al. [16] and shown in Figure 5.

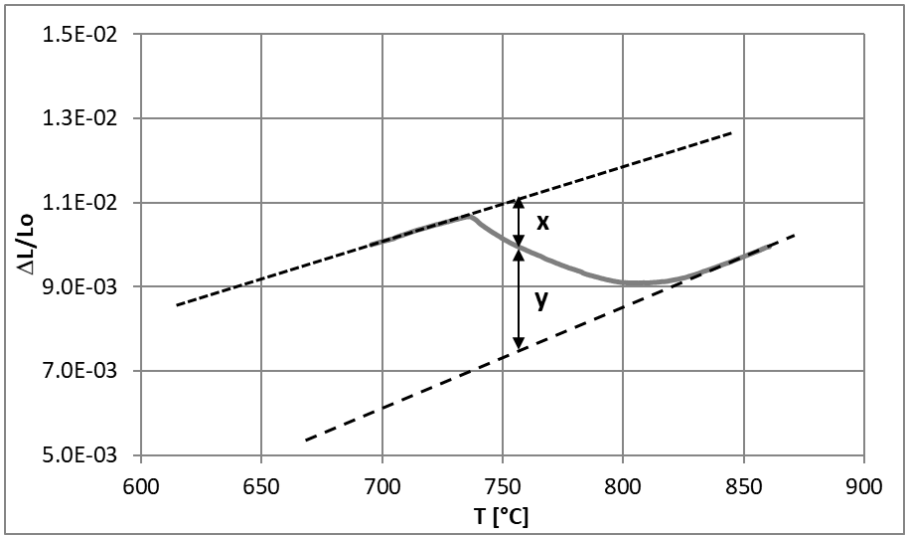

Figure 5. Procedure for the determination of the austenite fraction.

According to such procedure, the austenite fraction for a certain time and temperature is given by Equation 1:

$$\gamma\ [\%] = \frac{x}{x+y} \cdot 100 \qquad (1)$$

The austenite fractions versus time are compared in Figure 6.

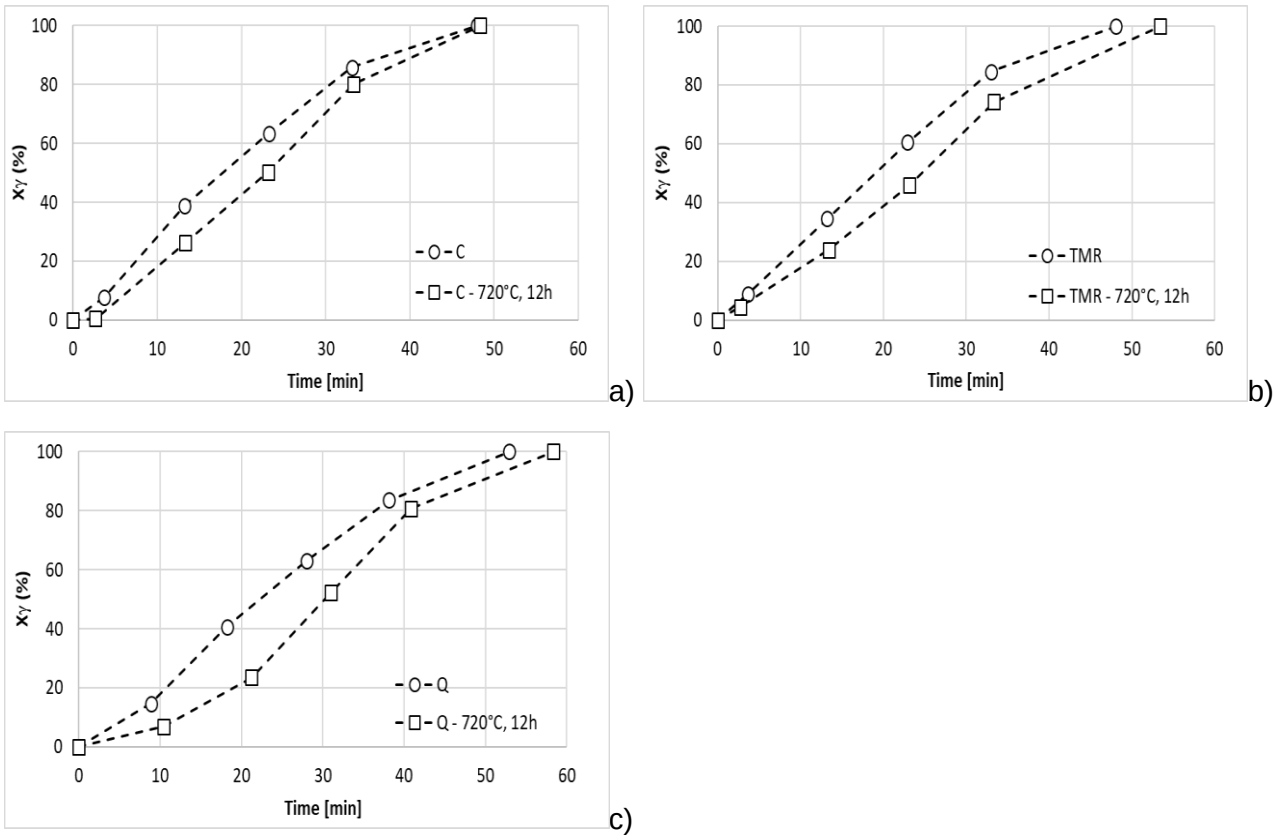

Figure 6. Comparison among the austenitization kinetics of as-produced and 720 °C, 12 h treated samples.

The graphs in Figure 6 confirm that spheroidal carbides slow down the austenite transformation. The observed differences can further increase in case of a real industrial heating, generally faster than the one chosen for these tests, i.e. 2 K/min.

3.2 Mechanical tests

The annealing kinetics was preliminarily studied by hardness tests. Then, the mechanical resistance and the deformability was determined on selected conditions by tensile tests. Figure 7 reports the hardness evolution during the spheroidization treatments.

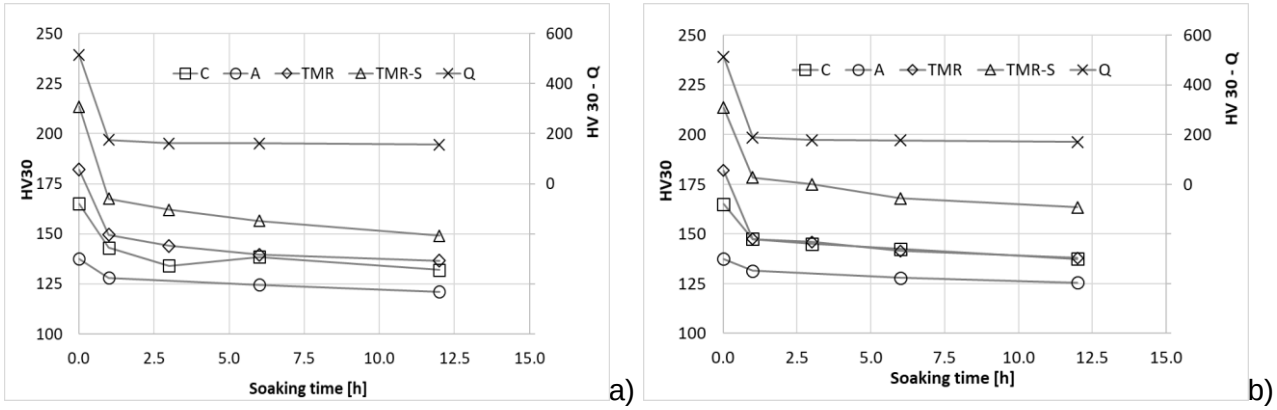

Figure 7. Evolution of the hardness values varying the soaking time at 720 °C (a) and 690 °C (b). The standard deviation for all the hardness measurements was lower than 5 HV30.

For both the temperatures, the hardness decreases quickly and already after 1h it is very close to the 12h soaking one. The loss of hardness after the first hour can hence be considered as an index

of the microstructure responsiveness when exposed to the annealing temperature. Figure 8 shows the calculated rates.

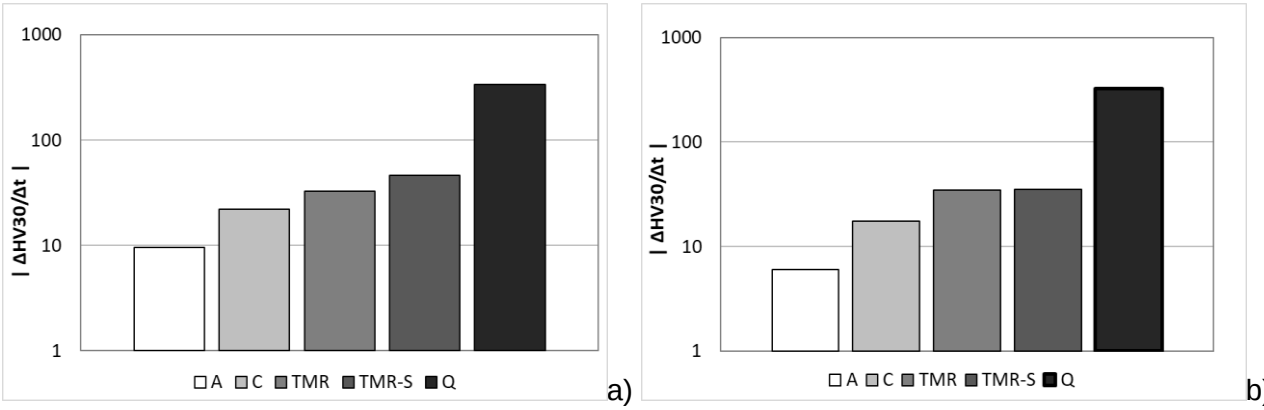

Figure 8. Hardness loss after 1 h soaking at 720 °C (a) and 690 °C (b).

For both the treatment temperatures, the slowest material is the one showing the coarsest pearlite (condition A). As the pearlite gets finer (conditions C and TMR), the loss of hardness is faster. The bainite (condition TMR-S) proved even more responsive than fine pearlitic microstructure, probably due to the morphology of the carbides that, differently from the lamellae, don't need to be chipped as required by the spheroidizing mechanisms described in the technical literature [17,18]. Martensite (condition Q) resulted the most responsive microstructure, even if it must be remarked that the mechanisms of carbides formation is completely different from the other microstructures and that its unstable condition gives a huge contribution to the reaction rate. It was anyway included in this work since it represents the most uniform carbon distribution in the metal matrix.

Hardness is commonly used for a preliminary evaluation of the mechanical resistance, but it cannot give information about the material deformability. Moreover, such parameter is generally not strictly related with the yield strength that is instead important to characterize the plastic behavior of a material. For such reasons, tensile tests were performed on samples treated at both the annealing temperatures for selected soaking times. Figures 9 and 10 show the results of the tensile tests for specimens treated at 720 °C and 690 °C respectively.

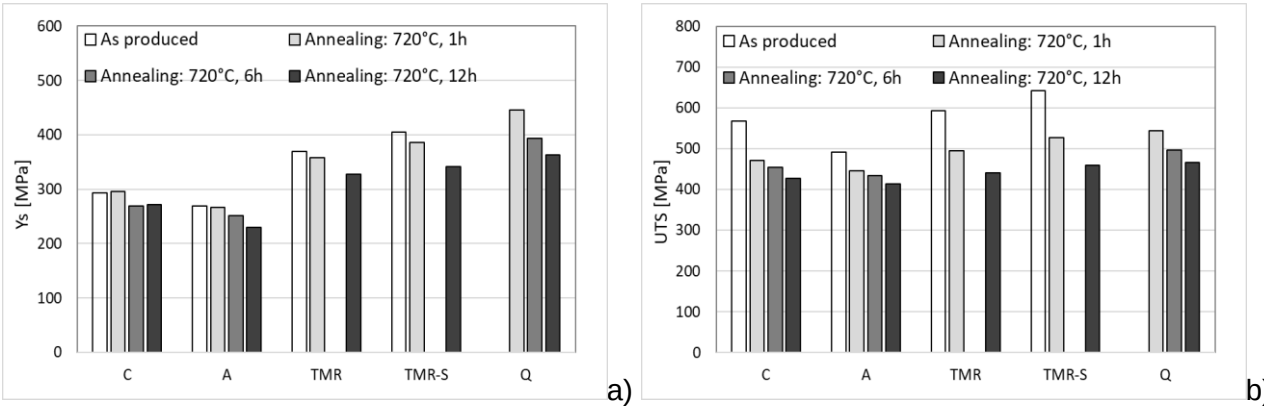

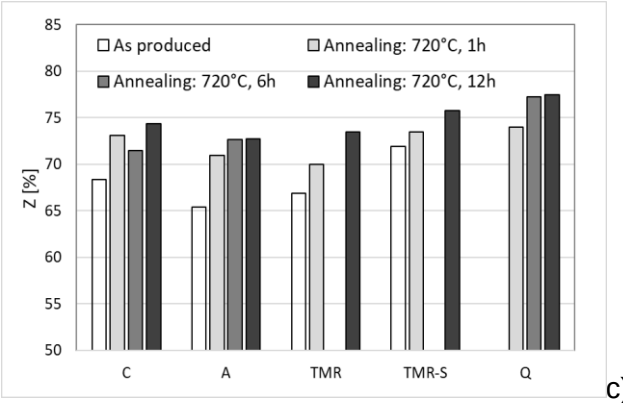

c)

Figure 9. Yield strength (a), UTS (b) and reduction of area (c) for specimens treated at 720 °C varying the soaking time.

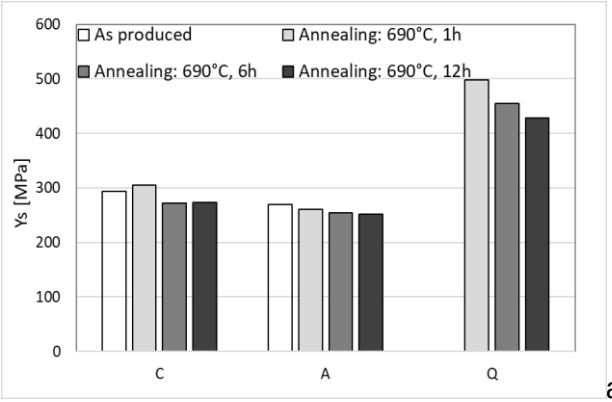

a)

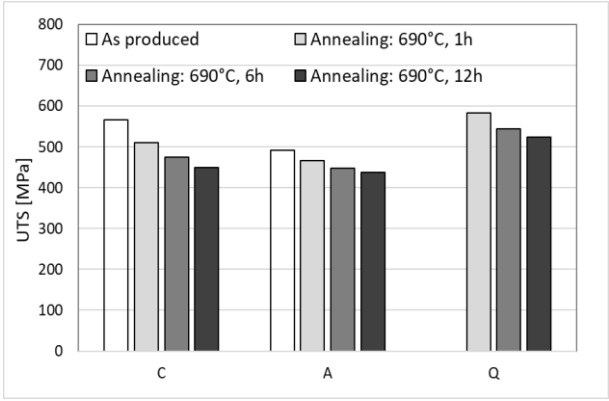

b)

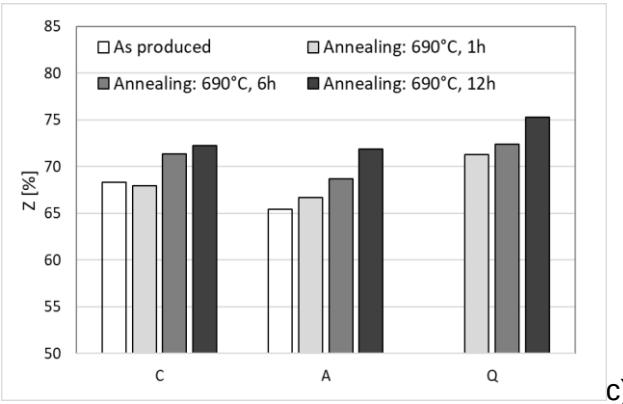

c)

Figure 10. Yield strengths (a), UTS (b) and reduction of area (c) for specimens treated at 690 °C varying the soaking time.

The data in Figures 9 and 10 show that, at both the annealing temperatures, the yield strength and the UTS decrease progressively as the spheroidization process goes on, whereas, as expected, the reduction of area improves. Since the transformation of the lamellar carbides into spheroidal ones depends on time and temperature, the tensile properties of the non-martensitic microstructures were studied as function of the Larson-Miller parameter described by Equation 2:

$$P_{LM} = T \cdot (K + \log(t)) \qquad (2)$$

T is the annealing temperature in Kelvin, t is the soaking time in hours and K is a constant.

As known, the yield strengths, the UTS and the reduction of area tend to a steady value for infinite soaking time. Such parameters can be described by the exponential laws reported in Equations 3, 4 and 5:

$$\frac{UTS}{UTS_0} = A_1 e^{B_1 \cdot P_{LM}} + \frac{UTS}{UTS_0}\Big|_\infty \quad (3)$$

$$\frac{Ys}{Ys_0} = A_2 e^{B_2 \cdot P_{LM}} + \frac{Ys}{Ys_0}\Big|_\infty \quad (4)$$

$$\frac{Z_0}{Z} = A_3 e^{B_3 \cdot P_{LM}} + \frac{Z_0}{Z}\Big|_\infty \quad (5)$$

UTS_o, Ys_o and Z_o are the as-produced tensile properties, whereas the index "∞" indicates the steady values. The parameters reported in Equations 3, 4 and 5 were determined by best fitting of the available data and are reported in Table 4.

K	A_1	B_1	$UTS/UTS_0\|_\infty$	A_2	B_2	$Ys/Ys_0\|_\infty$	A_3	B_3	$Z_0/Z\|_\infty$
1	0.27	$-5.85 \cdot 10^4$	0.73	0.22	$-3.91 \cdot 10^4$	0.80	0.15	$-3.59 \cdot 10^4$	0.85

Table 4. Parameters included in Equations 2, 3, 4 and 5.

The experimental and the calculated data are in good agreement as visible in Figure 11.

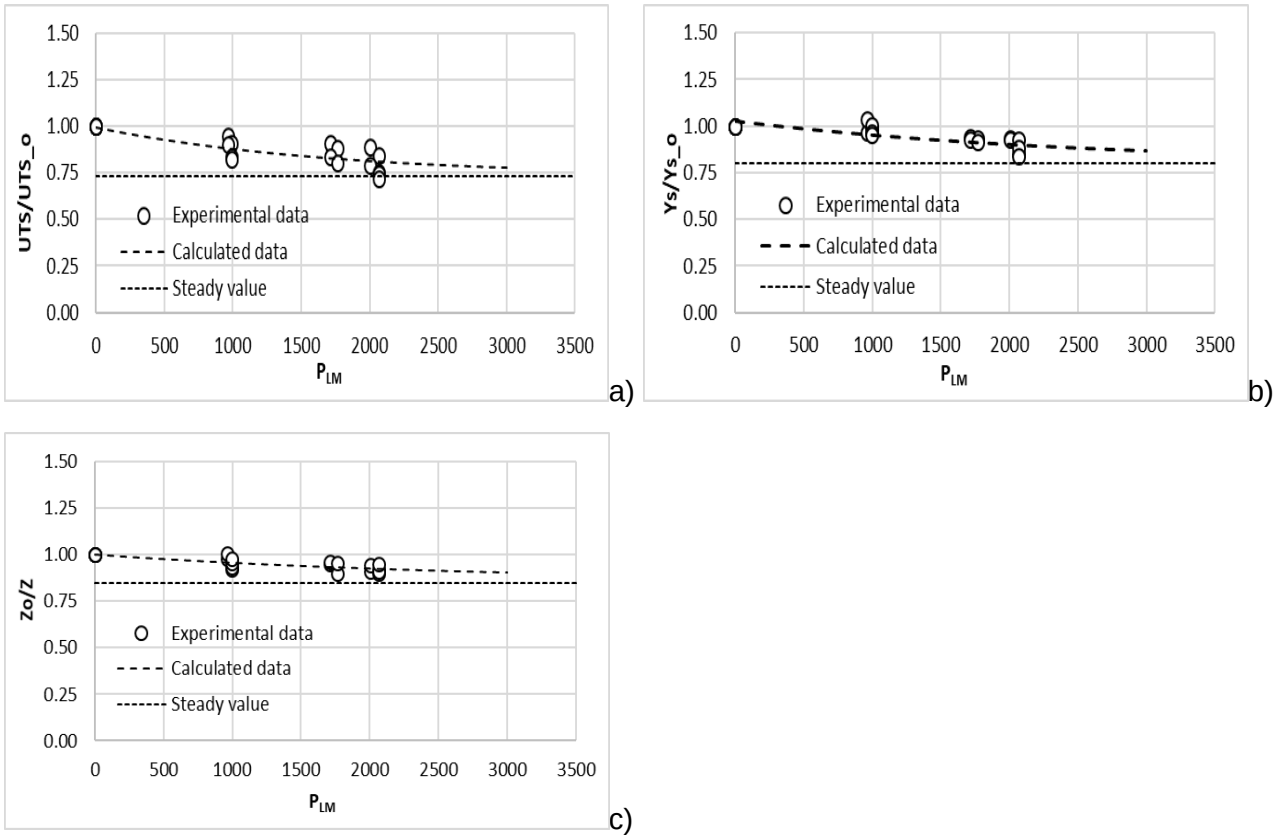

Figure 11. Comparison among the experimental and the calculated data.

From Equations 3, 4 and 5, the knowledge of the as-produced characteristics, UTS_o, Ys_o and Z_o, allows the calculation of the mechanical properties under specific time-temperature conditions. They fit well the experimental data as demonstrated by the graphs in Figure 12 and by the average absolute errors reported in Table 5.

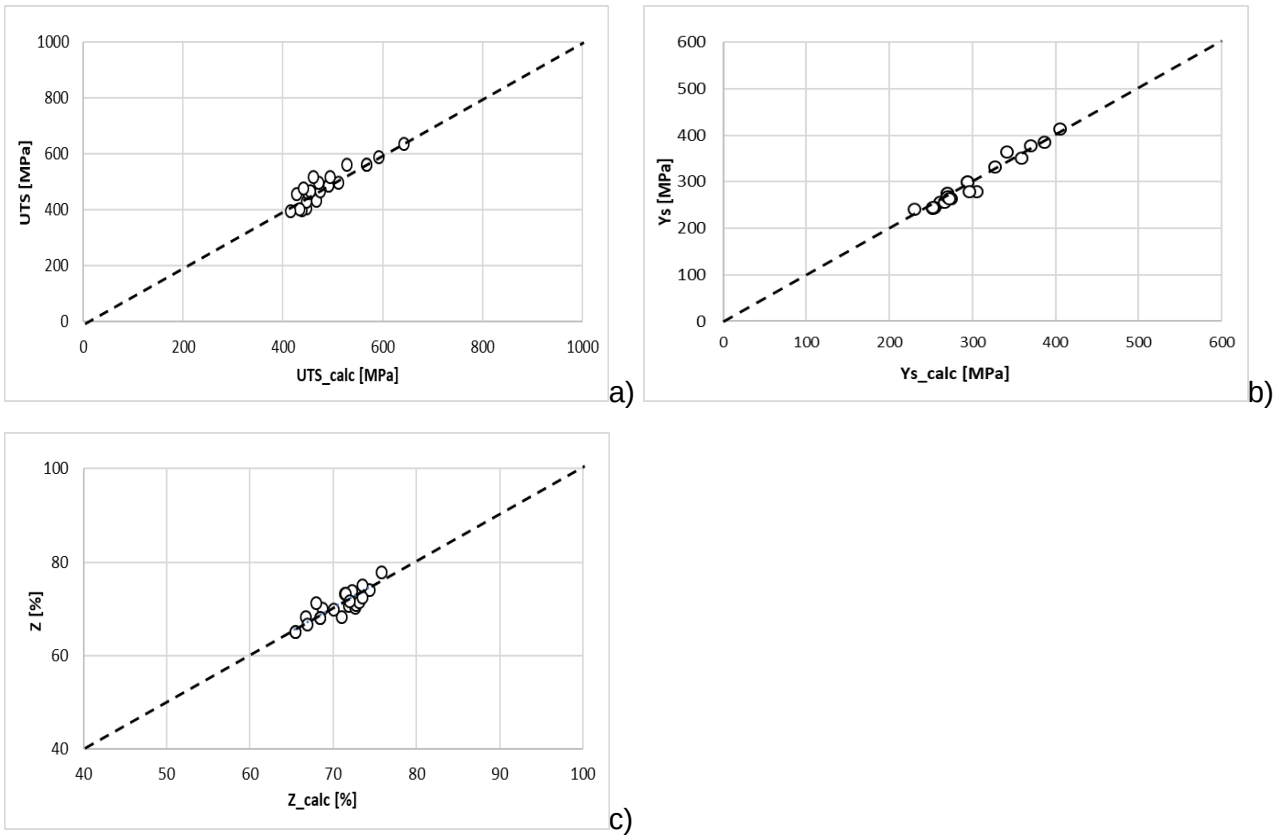

Figure 12. Comparison among the experimental and the calculated UTS, Ys and Z data.

	UTS	YS	Z
Average Abs. Error [%]	4.4	2.9	1.8
Standard Dev. [%]	3.6	2.0	1.4

Table 5. Average absolute errors and standard deviations associated to the calculation of the tensile properties.

Finally, to study the material plastic behaviour, the yield strength and the reduction of area values were combined in a chart as function of the prior microstructure and reported in Figure 13.

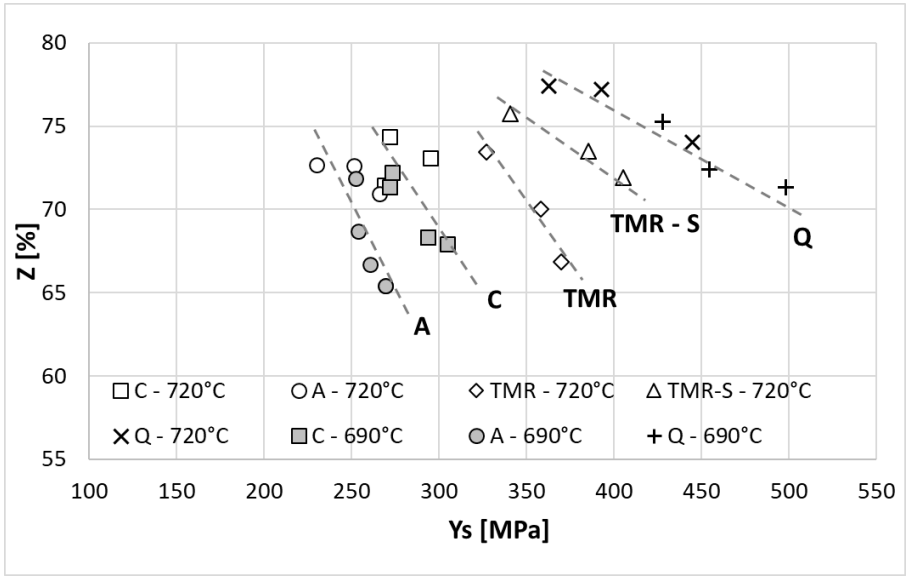

Figure 13. Reduction of area as function of the yield strengths for both the 690 °C and 720 °C treatments data.

Figure 13 shows that, for each prior microstructure, there is a linear relation between the deformability and the yield strengths. Moreover, the data occupy a precise region in the graph, function of the corresponding original structure. The worst combination of yield strength and reduction of area belongs to the coarsest microstructure (condition A), whereas the quenched and annealed specimens (condition Q) are characterized by the best behavior. Regarding the ferritic and pearlitic matrixes, the finer the microstructure, the higher the Ys/Z ratio. The bainitic matrix (condition TMR-S) showed a good behavior, included among the fine ferrite and pearlite and the tempered martensite structures. The data in Figure 13 demonstrate that for a fixed value of the deformability, the right choice of the prior microstructure can give also high yield strengths. This property can be exploited during industrial plastic deformations, since it can reduce the number of stages necessary to reach a specific mechanical resistance or, without any modification to the existing set-up, to obtain a product with a superior resistance.

Conclusions

The present experimental work studied the relation among the deformability and the mechanical resistance of a low-carbon boron steel subjected to different spheroidizing treatments. The microstructural observations confirmed that the carbides shape and size depend on the annealing temperature and time, being the change of carbides morphology faster for higher treatment temperature. The carbides dispersion in the metal matrix is instead strongly related to the prior microstructure: a more uniform distribution of carbon in the matrix, such as the one of the bainitic and martensitic structures, results in a better arrangement of the carbides with a positive consequence on the deformability. The tests confirmed that also the response of the material to the annealing temperature, is function of the prior microstructure: after the martensitic matrix, the bainitic microstructure proved more responsive in respect to the ferrite-pearlite structures. Nevertheless, it's important to remark that fine pearlite, such as the one obtained by thermomechanical rolling, showed a quicker kinetics in respect to coarser structures. As already reported in the technical literature, the dilatometric analysis confirmed that the spheroidal pearlite has a slower $\alpha \rightarrow \gamma$ transformation. This can become critical during the quenching stage, especially when the heating rate is high, since it can be responsible of an incomplete solution of the carbides in the austenitic matrix.

The comparison between the reduction of area and the corresponding yield strength demonstrates that it is possible to obtain good deformability even if the mechanical resistance is not minimized. This can be exploited in industrial processes to get superior performances or a simplified production cycle.

The deformability at 690°C is lower than the 720 °C one, but it is anyway good being the reduction of area only about 4 % less for all the tested initial conditions. This suggests that also lower annealing temperatures can be suitable for cold forming operations if the prior microstructure is properly selected. Nevertheless, a further important issue that must be studied, is the relation among the reduction of area and the formability of the material during real plastic deformations. The encouraging results obtained in this work suggest and justify future formability tests in collaboration with companies operating in the cold-deformation field, to confirm that the laboratory analysis can really lead to innovative industrial products.

References

[1] M. Nikravesh, M. Naderi, G.H. Akbari, W. Bleck, Phase transformations in a simulated hot stamping process of the boron bearing steel, Materials and Design 84 (2015) 18–24.

[2] Anjana Deva, Saikat K. De, Vinod Kumar, M. Deepa, B.K. Jha, Influence of Boron on the Hardenability of Unalloyed and Low Alloyed Steel, International Journal of Metallurgical Engineering 2013, 2(1): 47-51.

[3] N. J. Bradley, R. I. Stephens, N. J. Horn, J. J. Gradman, J. M. Arkema, and C. S. Borgwardt, Influence of Cold Rolling Threads before or after Heat Treatment on the Fatigue Resistance of High Strength Fine Thread Bolts for Multiple Preload Conditions, Journal of ASTM International, April 2006, Vol. 3, No. 4

[4] Marcelo A.L., Uehara A.Y., Utiyama R.M., Ferreira I., Fatigue Properties of High Strength Bolts, ICM 11 Procedia Engineering 10 (2011) 1297–1302.

[5] Erdal Karadeniz, Influence of different initial microstructure on the process of spheroidization in cold forging, Materials and Design 29 (2008) 251–256.

[6] YIYOU TU, LINGHUI HUANG, XIAOHUI WANG, XUEFENG ZHOU, FENG FANG, JIANQING JIANG, Effect of Si and Mn Interactions on the Spheroidization and Coarsening Behaviour of Cementite During Annealing in Severe Cold-Drawn Pearlitic Steel, Metallurgical and materials transactions A, November 2015, DOI: 10.1007/s11661-015-3219-3.

[7] Vv.Aa, Heat Treating, ASM Handbook, Volume 4. Steel Heat Treating Fundamentals and Processes Editor: Jon Dossett and George E. Totten, ASM, Metals Park, 2013.

[8] R. Allen Schaneman, The Effects of Prior Microstructure on Spheroidizing Kinetics and Cold Workability in Bar Steels, Colorado School of Mines, 2009.

[9] Hoon Hwang and Bruno C. De Co, Influence of the Initial Microstructure on the Spheroidization of SAE 52100 Bearing Steel, steel research int. 87 (2016) No. 1

[10] Ata Karnyabi-Gol', Meisam Sheikh-Amid, Spheroidizing Kinetics and Optimization of Heat Treatment Parameters in CK60 Steel Using Taguchi Robust Design, Journal of iron and steel research international, 2010, 17(4): 45-52

[11] Yu. P. Gul’, M. A. Sobolenko, and A. V. Ivchenko, Improvement in the Spheroidizing Annealing of Low Carbon Steel for Cold Upsetting, Steel in Translation, 2012, Vol. 42, No. 6, pp. 531–535

[12] B. Rivolta, R. Gerosa, C. Sala, F. Tavasci, L. Angelini, N. Bolognani, A. Panzeri, A. Parimbelli, Influence of prior microstructure on the mechanical and microstructural properties of C–Mn–B steel after spheroidizing annealing, Ironmaking & Steelmaking, DOI: 10.1080/03019233.2020.1858223.

[13] H. Paqueton, A. Pineau, Acceleration of pearlite spheroidization by thermomechanical treatment, Journal of the iron and steel institute, 1971.

[14] Henrique Duarte Alvarenga, Nele Van Steenberge, Jilt Sietsma, Herman Terryn, The Kinetics of Formation and Decomposition of Austenite in Relation to Carbide Morphology, METALLURGICAL AND MATERIALS TRANSACTIONS A, VOLUME 48A, FEBRUARY 2017.

[15] Mattia Spezzapria, Alessio G. Settimi, Luca Pezzato, Michele F. Novella, Michele Forzan, Fabrizio Dughiero, Stefania Bruschi, Andrea Ghiotti, Katya Brunelli, Manuele Dabalà, Effect of Prior Microstructure and Heating Rate on the Austenitization Kinetics of 39NiCrMo3 Steel, steel research int. 88 (2017) No. 5.

[16] Huiping Li, Kang Gai, Lianfang He, Chunzhi Zhang, Hongzhi Cui, Musen Li, Non-isothermal phase-transformation kinetics model for evaluating the austenitization of 55CrMo steel based on Johnson–Mehl–Avrami equation, Materials and Design, 92, (2016), 731–741.

[17] Y. L. Tian and R. W. Kraft, "Mechanisms of Pearlite Spheroidization," Metallurgical Transactions A, vol. 18A, 1987, pp. 1403-1414.

[18] S. Chattopadhyay and C. M. Sellars, "Kinetics of Pearlite Spheroidization During Static Annealing and During Hot Deformation," Acta Metallurgica, vol. 30, 1982, pp. 157-170.